

# The catabolic pathways of *in situ* rhizosphere PAH degraders and the main factors driving PAH rhizoremediation in oil-contaminated soil

Jibing Li <sup>1,2</sup> Chunling Luo <sup>1,2,3\*</sup> Dayi Zhang <sup>4</sup>,  
Xuan Zhao,<sup>1,5</sup> Yeliang Dai,<sup>1,5</sup> Xixi Cai<sup>6</sup> and  
Gan Zhang<sup>1,2</sup>

<sup>1</sup>State Key Laboratory of Organic Geochemistry and Guangdong-Hong Kong-Macao Joint Laboratory for Environmental Pollution and Control, Guangzhou Institute of Geochemistry, Chinese Academy of Sciences, Guangzhou 510640, China.

<sup>2</sup>CAS Center for Excellence in Deep Earth Science, Guangzhou 510640, China.

<sup>3</sup>Joint Institute of Environmental Research & Education, South China Agricultural University, Guangzhou 510642, China.

<sup>4</sup>College of New Energy and Environment, Jilin University, Changchun 130021, China.

<sup>5</sup>University of Chinese Academy of Sciences, Beijing 100039, China.

<sup>6</sup>Guangdong Key Laboratory of Environmental Catalysis and Health Risk Control, School of Environmental Science and Engineering, Institute of Environmental Health and Pollution Control, Guangdong University of Technology, Guangzhou 510006, China.

## Summary

**Rhizoremediation is a potential technique for polycyclic aromatic hydrocarbon (PAH) remediation; however, the catabolic pathways of *in situ* rhizosphere PAH degraders and the main factors driving PAH rhizoremediation remain unclear. To address these issues, stable-isotope-probing coupled with metagenomics and molecular ecological network analyses were first used to investigate the phenanthrene rhizoremediation by three different prairie grasses in this study. All rhizospheres exhibited a significant increase in phenanthrene removal and markedly modified the diversity of phenanthrene degraders by increasing their populations and interactions with**

**other microbes. Of all the active phenanthrene degraders, *Marinobacter* and *Enterobacteriaceae* dominated in the bare and switchgrass rhizosphere respectively; *Achromobacter* was markedly enriched in ryegrass and tall fescue rhizospheres. Metagenomes of <sup>13</sup>C-DNA illustrated several complete pathways of phenanthrene degradation for each rhizosphere, which clearly explained their unique rhizoremediation mechanisms. Additionally, propanoate and inositol phosphate of carbohydrates were identified as the dominant factors that drove PAH rhizoremediation by strengthening the ecological networks of soil microbial communities. This was verified by the results of rhizospheric and non-rhizospheric treatments supplemented with these two substances, further confirming their key roles in PAH removal and *in situ* PAH rhizoremediation. Our study offers novel insights into the mechanisms of *in situ* rhizoremediation at PAH-contaminated sites.**

## Introduction

Polycyclic aromatic hydrocarbons (PAHs) are a group of organic priority pollutants that are widely distributed in soils, sediments and air (Kuppusamy *et al.*, 2016). In the past several decades, there have been increasing concerns regarding the effects of PAHs on human health and ecosystem because of their potential toxicity and carcinogenicity (Li *et al.*, 2017). Rhizoremediation, which involves both plants and rhizosphere-associated microorganisms, is proposed as a promising, *in situ* and cost-effective alternative to minimize the consequences of soil PAH pollution (Wu *et al.*, 2018).

Plant rhizospheres play critical roles in improving the remediation efficiency of PAHs, and rhizospheric microorganisms are particularly important (Yu *et al.*, 2011; Li *et al.*, 2019b). Rhizosphere effects vary across plant species, soil types and indigenous microbes, consequently affecting rhizoremediation performance (Guo *et al.*, 2017). To explore the mechanisms underlying the effects of rhizospheres on PAH degradation, a wide range of plants including ryegrass (RG), tall fescue (TF),

Received 31 July, 2021; revised 15 September, 2021; accepted 24 September, 2021. \*For correspondence. E-mail clluo@gig.ac.cn; Tel. +86-20-85290290; Fax +86-20-85290706.

switchgrass (SG) and wheat have been used and uncovered some key microbial lineages and related functional genes (Chen *et al.*, 2003; Shahsavari *et al.*, 2015; Guo *et al.*, 2017; Li *et al.*, 2019b). Some recent studies have also attempted to explore the performance of active PAH degraders in the plant rhizosphere, which are critical for PAH rhizoremediation efficiency (Thomas *et al.*, 2019; Li *et al.*, 2019b). Our previous work found key contributions of the diversity of the active PAH degraders and functional PAH-degrading genes in RG rhizosphere to rhizoremediation efficiency (Li *et al.*, 2019b). However, the mechanisms of *in situ* PAH rhizoremediation are unclear; the catabolic pathways, interspecies relationships and factors influencing *in situ* PAH degraders in the metabolisation of PAHs remain unknown. Metagenomics have been widely used to elucidate the genomes of environmental microbes, allowing exploration of the potential functional capabilities and metabolic pathways of active degraders (Chen and Murrell, 2010; Thomas *et al.*, 2019). Additionally, molecular ecological network analyses (MENA) have been conducted to determine the complex interactions between active degraders and other members within the community (Song *et al.*, 2019). Combining these two approaches is helpful for solving the above-mentioned problems. Thus far, only one metagenomics study has successfully investigated the metabolic pathways responsible for *in situ* PAH remediation in the RG rhizosphere (Thomas *et al.*, 2019); to our knowledge, there is no evidence regarding the complex associations between PAH degraders and other microbes in rhizospheres, or elucidating the driving factors of PAH rhizoremediation, which hinders the understanding of PAH rhizoremediation mechanisms.

Although the investigation of *in situ* PAH degraders in the rhizoremediation process is of great significance for understanding the mechanism of rhizoremediation (Thomas *et al.*, 2019), it remains challenging to specifically target the active PAH degraders *in situ* by means of traditional pure culture techniques. These approaches do not truly reflect the actual roles of isolated microorganisms in the natural environment; most such microorganisms are uncultivable (Amann *et al.*, 1995). DNA-stable isotope probing (DNA-SIP) is a cultivation-independent technique that aims at linking metabolic functions to phylogenetic identities of microbes in complex microbial communities. This technique has been successfully used to identify the active PAH degraders in RG rhizosphere (Thomas *et al.*, 2019). The combination of DNA-SIP and metagenomics (SIP-metagenomics) enables a better understanding of the degradation mechanisms of many pollutants (Chen and Murrell, 2010). However, few studies have investigated the mechanisms of PAH degradation using this technique (Rochman *et al.*, 2017; Thomas *et al.*, 2019). To our knowledge, only one study has

explored the mechanisms underlying microbial degradation of *in situ* PAH rhizoremediation in RG rhizospheres (Thomas *et al.*, 2019); that study did not ascertain the main factors that drive PAH degraders in PAH-contaminated rhizospheres. Thus, there is a lack of evidence regarding the rhizosphere effects of different plant species on the PAH degrader community, as well as and the main factors driving PAH rhizoremediation. This is especially critical for selecting the most suitable plants for PAH rhizoremediation, thus improving remediation performance.

Phenanthrene (PHE) is a typical model compound used to study PAH biodegradation because of its ubiquitous nature and fused-ring angular structure (Seo *et al.*, 2009; Luo *et al.*, 2021). Here, we selected <sup>13</sup>C-labelled PHE as a metabolic tracer and first applied SIP-metagenomics and MENA to compare the influences of different plant rhizospheres (RG, TF, SG) on the structure, diversity and metabolic features of the active PHE-degrading microbial communities, discuss their correlations with other members, and explore the driving factors of PAH rhizoremediation. We hypothesised that plant rhizospheres could improve the PHE rhizoremediation performance by changing the metabolic pathways of the active PHE degraders and specific carbohydrates in the rhizosphere might drive the active degraders *in situ* to metabolize PHE. The objectives of this work were to identify the active PHE degraders and their catabolic pathways, and determine the influential factors driving PHE rhizoremediation by different plants to clean PAH-polluted soils. We hope that this study will offer new insights regarding the mechanisms of PAH rhizoremediation and provide useful information to enhance the PAH rhizoremediation efficiency in PAH-containing soils.

## Results

### Biodegradation of PHE

The elimination of PHE after 12 days is illustrated in Fig. 1. The recovery rates of PHE during the extraction procedure were 75%–85% in this study. Minimal PHE was detected in the tissues of different prairie grasses over the 12-day period (data not shown). All biotic treatments showed significant PHE removal performance; however, more than 89.4% of PHE remained in the abiotic microcosms (CK), indicating the occurrence of PHE biodegradation. All planted treatments exhibited a significant decline of PHE concentration ( $p < 0.05$ ). PHE degradation efficiency was significantly different between each of the planted treatments (RG, TF or SG) and the unplanted control (AD) after a 12-day incubation ( $p < 0.05$ , Fig. 1). More precisely, there was 25.7%,

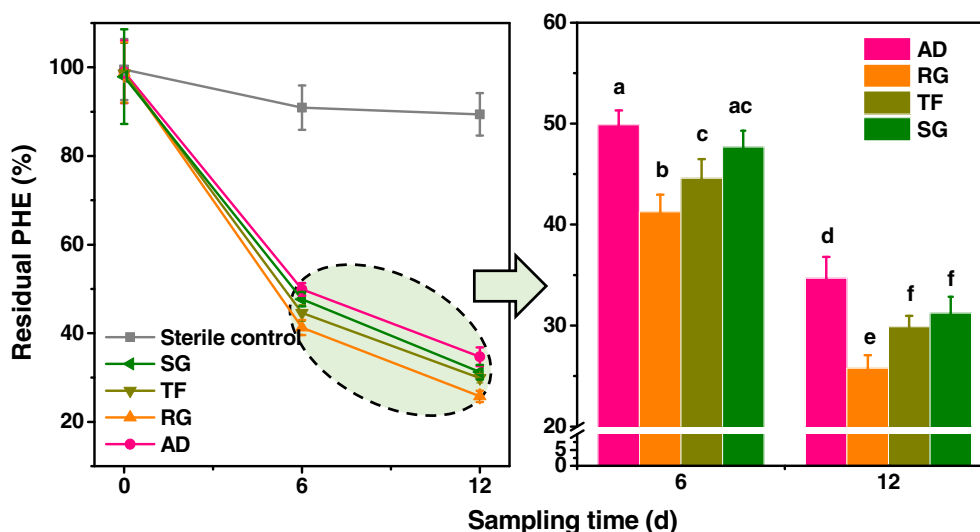


**Fig. 1.** Residual PHE percentage in AD, RG, TF and SG microcosms. Data are means  $\pm$  standard deviation;  $n = 3$ . [Color figure can be viewed at [wileyonlinelibrary.com](http://wileyonlinelibrary.com)]

29.8% and 31.2% of residual PHE in the RG, TF and SG microcosms after 12-day incubation; however, 34.7% of PHE remained in the unplanted AD treatment. Among all plants, RG exhibited the highest PHE degradation efficiency, followed by TF and SG.

#### Soil bacterial populations and community composition

Results from qPCR and 16S rRNA gene amplicon sequencing suggested that the total abundances of 16S rRNA gene in RG ( $6.46 \times 10^8$  copies  $g^{-1}$  soil), TF ( $6.43 \times 10^8$  copies  $g^{-1}$  soil) and SG microcosms ( $6.14 \times 10^8$  copies  $g^{-1}$  soil) were approximately 17-fold higher than that in AD microcosms ( $5.59 \times 10^7$  copies  $g^{-1}$  soil) after the 12-day degradation (Fig. S1). From the bacterial community composition in all biotic treatments (Fig. S2), there were no obvious difference in the composition and structure of the soil bacterial community between samples amended with  $^{12}C$ -PHE and  $^{13}C$ -PHE over the 12-day period ( $p > 0.05$ ), whereas distinct changes were observed in some microbes between the unplanted and planted treatments. For example, dominant bacteria such as members of the unclassified OM1 clade, *Pseudomonas*, *Marinobacter* and *Desulfuromonas* were detected in all treatments, and their relative abundances significantly declined in the planted microcosms on days 6 and 12 comparing to the unplanted treatments.

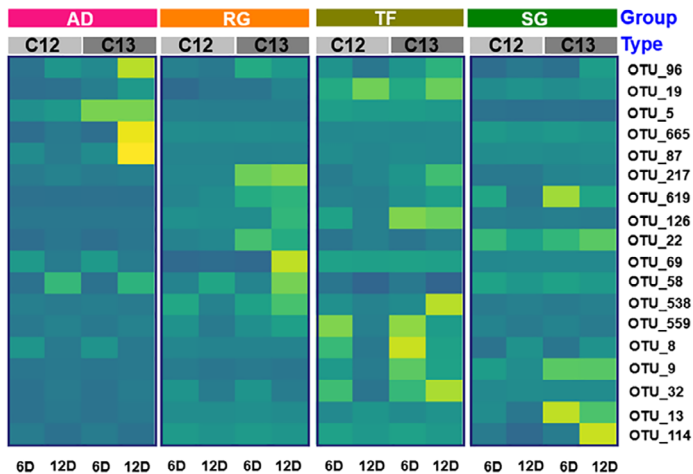
#### Taxonomic characterization of the active PHE degraders in unplanted and planted treatments

Based on the qPCR results, bacterial 16S rRNA genes were significantly enriched in the fractions with high buoyant density (BD, 1.7556–1.7567  $g\ ml^{-1}$ ) of  $^{13}C$ -AD

microcosms; thus, these fractions were selected as the 'heavy' DNA fractions ( $^{13}C$ -DNA) of  $^{13}C$ -AD microcosms (Fig. S3). Additionally, the active PHE degraders assimilating  $^{13}C$ -PHE were further determined by comparing the relative abundances of operational taxonomic units (OTUs) in each fraction of  $^{12}C$ -AD and  $^{13}C$ -AD treatments (Li *et al.*, 2017). Here, the active PHE degraders represented by five OTUs were enriched in the heavy DNA fractions of  $^{13}C$ -AD treatments, but no enrichment was detected in the  $^{12}C$ -AD treatment (Figs 2 and S4), hinting the critical roles of these microorganisms in the *in situ* PHE degradation in the unplanted treatments.

All planted treatments significantly changed the diversity and composition of the active PHE degraders (Fig. 2). In RG microcosms, microbes represented by 10 OTUs were determined as the active PHE degraders (Figs 2 and S5). For TF and SG treatments, nine and seven OTUs were responsible for the *in situ* PHE rhizoremediation respectively (Figs 2, S6 and S7). Details for the identification of OTUs representing the active PHE degraders are provided in the Supporting Information. The specific taxonomies of the identified active degraders and their similarities to the closest microorganisms are listed in Table S3. They were affiliated with eight bacterial classes: *Alphaproteobacteria*, *Betaproteobacteria*, *Gammaproteobacteria*, *Deltaproteobacteria*, *Verrucomicrobia*, *Bacilli*, *Actinobacteria* and *Thermomicrobia*. Among them, *Marinobacter* (OTU\_5) in the unplanted treatments (AD), *Achromobacter* (OTU\_217; RG and TF) and *Enterobacteriaceae* (OTU\_13; SG) in the planted treatments were significantly enriched in the heavy DNA fractions with high abundance (>1%) (Fig. 2), indicating their dominant position and key roles in PHE removal. Additionally, the phylogenetic positions of the active PHE

A



B

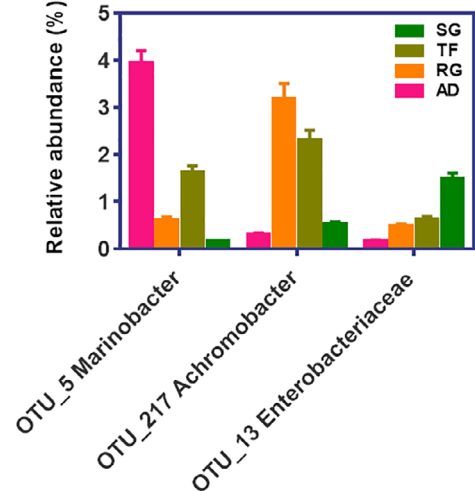


**Fig. 2.** (A) Heatmap of key OTUs in the heavy DNA fractions from the AD, RG, TF and SG treatments. Colours indicate the relative abundance, ranging from purple (low) to yellow (high). 6D and 12D represent soils collected on days 6 and 12 respectively. C12 and C13 refer to samples amended with  $^{12}\text{C}$ -phenanthrene and  $^{13}\text{C}$ -phenanthrene respectively. Values are means of three independent replicates. (B) OTUs (>1%) significantly enriched in the heavy DNA fractions from the  $^{13}\text{C}$ -AD,  $^{13}\text{C}$ -RG,  $^{13}\text{C}$ -TF and  $^{13}\text{C}$ -SG treatments after 12-day incubation, comparing to the  $^{12}\text{C}$ -AD,  $^{12}\text{C}$ -RG,  $^{12}\text{C}$ -TF and  $^{12}\text{C}$ -SG treatments. Values are mean  $\pm$  standard deviation ( $n = 3$ ). [Color figure can be viewed at [wileyonlinelibrary.com](http://wileyonlinelibrary.com)]

degraders indicated the significant effects of plant rhizospheres on their composition and diversity (Fig. 3).

#### Correlations of bacterial abundance with PHE degradation efficiency

To explore the possible connections among soil bacteria, active PHE degraders and PHE degradation efficiency, the Pearson correlation analysis was conducted (Figs S9 and S10). PHE degradation efficiency was positively correlated with the number of the active PHE degraders ( $r = 0.951$ ,  $p < 0.05$ ) rather than total soil bacteria (Table S4), indicating the contribution of the active PHE degraders to the *in situ* rhizoremediation of PAH-contaminated soils.

#### $^{13}\text{C}$ -DNA metagenomes and their relationships with PHE degradation efficiency

Based on the KEGG database, we compared the metabolic profiles of active PHE degraders from the unplanted and planted treatments. As shown in Fig. 4, 20 of 27 functional categories exhibited differently in the four treatments. In categories with relative abundance >5%, the difference in carbohydrate metabolism was greatest between treatments (12.09%, 12.79%, 13.22% and 15.07% in the  $^{13}\text{C}$ -DNA metagenomes of AD, RG, TF and SG treatments respectively;  $q$ -value < 0.001). In the 14 carbohydrate metabolism categories, the abundances of genes related to the metabolisms of starch, sucrose,

pyruvate, pentose phosphate, glyoxylate and dicarboxylate were higher in the  $^{13}\text{C}$ -DNA metagenomes of the planted treatments (Fig. 4B). Furthermore, there were significant differences in xenobiotic biodegradation and metabolism (including aromatic compound biodegradation) between the unplanted and planted treatments (11.20%, 10.01%, 8.72% and 8.05% in the  $^{13}\text{C}$ -DNA metagenomes of AD, RG, TF and SG treatments respectively;  $q$ -value = 0.014). Particularly within the category of xenobiotic biodegradation and metabolism (Fig. 4C), the subcategories of PAH degradation, as well as naphthalene, toluene and xylene degradation, were underrepresented in the  $^{13}\text{C}$ -DNA metagenomes of the planted treatments.

To explore the associations between substance metabolism of  $^{13}\text{C}$ -DNA metagenomes and degradation efficiency, and then discuss the potential drivers of PAH biodegradation in rhizospheres, we analysed the correlations regarding the metabolism of two categories (carbohydrate and xenobiotic biodegradation and metabolism) and their subcategories with PHE degradation efficiency. Surprisingly, we did not observe a significant correlation (Fig. 5A); however, significant positive correlations were observed between PHE degradation efficiency and gene sequences affiliated to propanoate (Pr) ( $r = 0.87$ ,  $p < 0.05$ ) and inositol phosphate (IP) metabolisms ( $r = 0.88$ ,  $p < 0.05$ ) within carbohydrate metabolism (Fig. 5B), indicating the importance of Pr and IP metabolisms in PHE rhizoremediation. Considering the strong association between the number of the active PHE

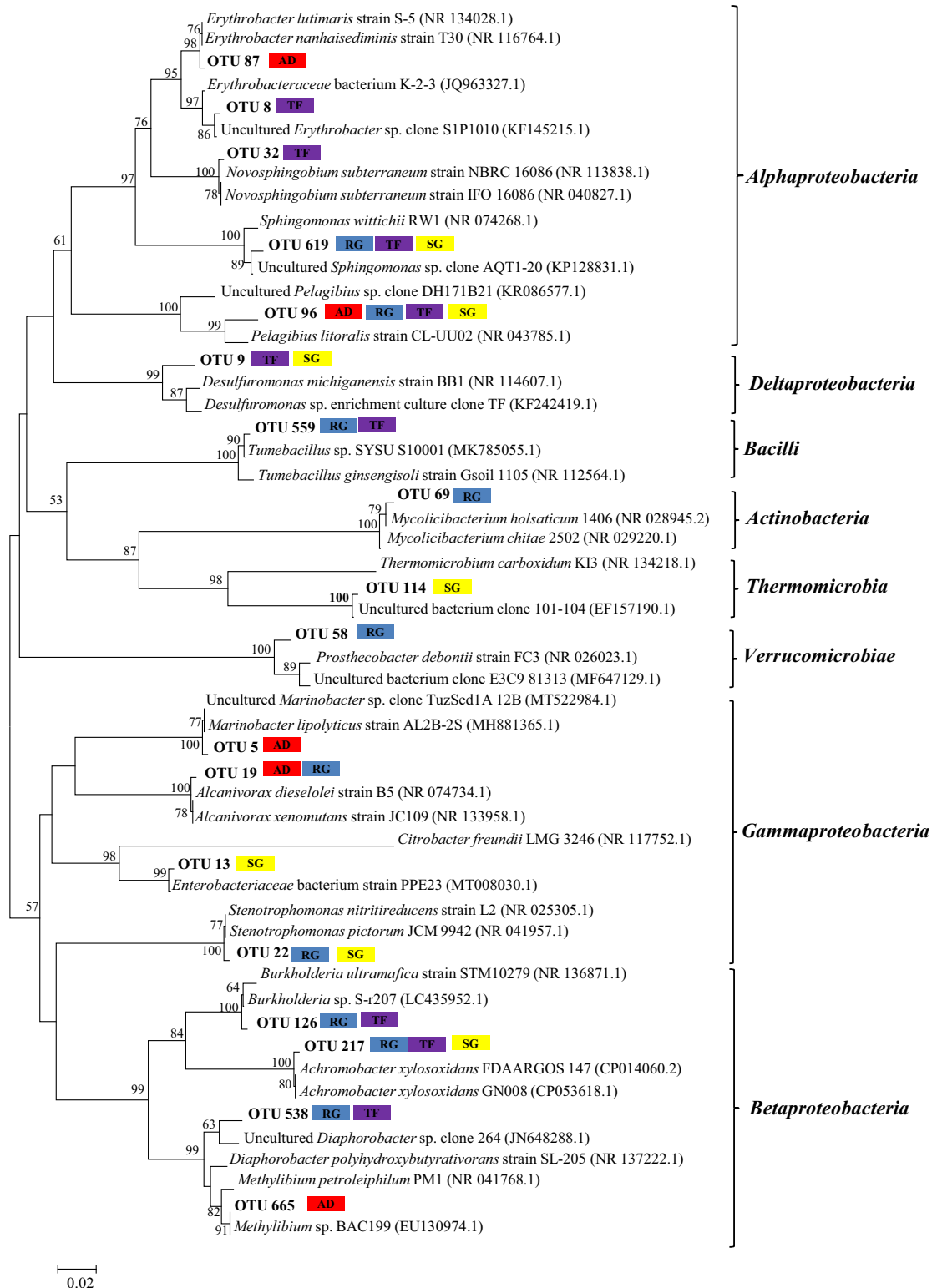


**Fig. 3.** Phylogenetic tree of OTUs responsible for *in situ* phenanthrene degradation based on the neighbour-joining method using 16S rRNA gene sequences. Bootstrap values >50% are shown at the branch points and bar represents 0.02 substitutions per nucleotide position. The active phenanthrene degraders identified from AD, RG, TF and SG treatments are highlighted in red, blue, purple and yellow colour respectively. [Color figure can be viewed at [wileyonlinelibrary.com](http://wileyonlinelibrary.com)]

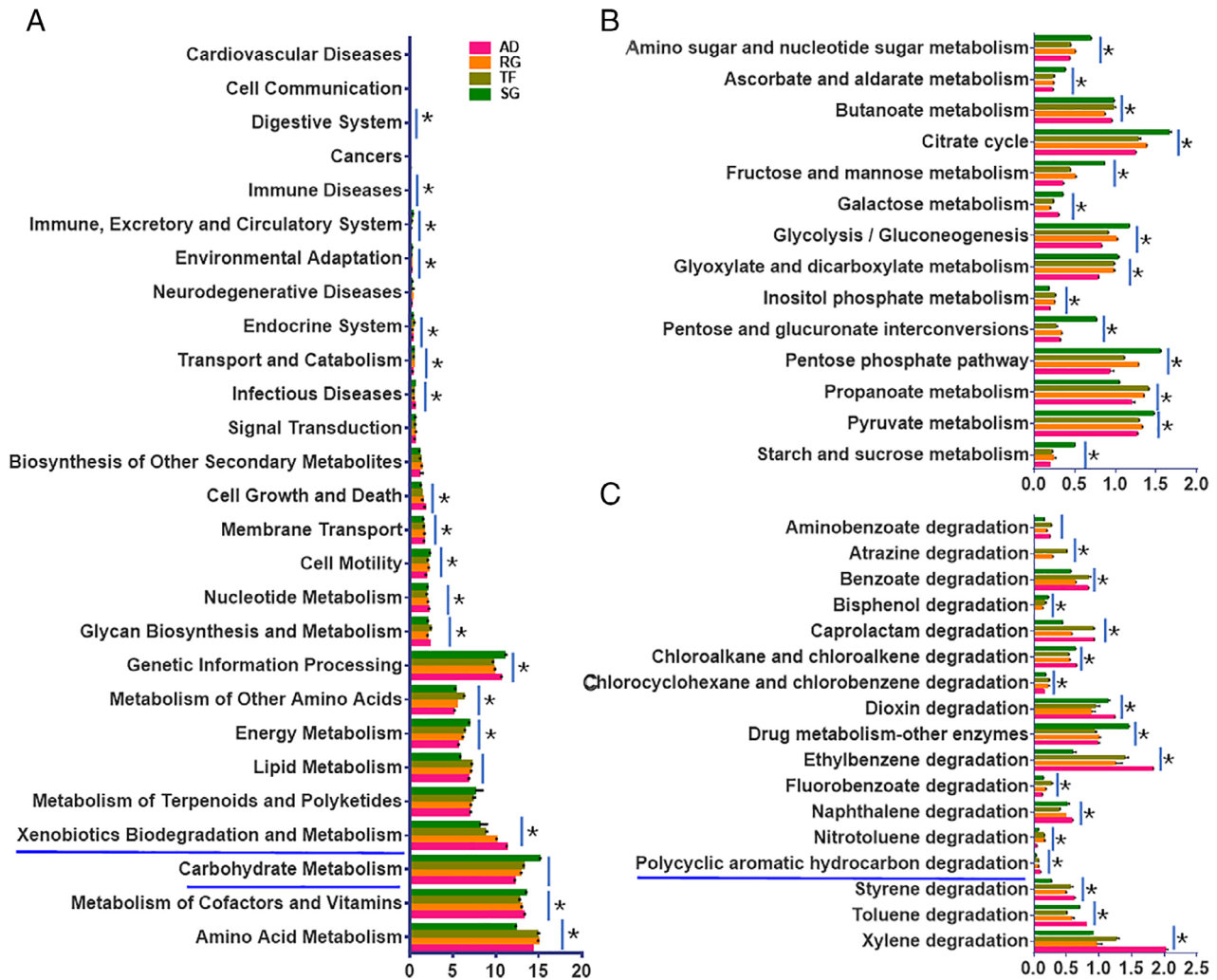


**Fig. 4.** Functional analysis of shotgun metagenomic aligned sequences in the heavy DNA of the unplanted and planted treatments amended with  $^{13}\text{C}$ -PHE (mean  $\pm$  standard deviation,  $n = 3$ ) based on the KEGG pathway database. The relative abundance of 27 functional categories (A), 14 carbohydrate metabolism categories (B), and 15 functional categories related to the xenobiotics biodegradation and metabolism (C). Only sub-categories with significant differences are shown. Asterisks indicate statistically significant differences ( $q$ -values  $< 0.05$  after Benjamini–Hochberg correction) between treatments. [Color figure can be viewed at [wileyonlinelibrary.com](http://wileyonlinelibrary.com)]

degraders and the degradation efficiency, the correlations between the active PHE degraders and metabolic genes related to Pr/IP were subjected to further analysis (shown in Fig. S11). Obviously, the metabolisms of Pr ( $r > 0.99$ ,  $p < 0.001$ ) and IP ( $r > 0.99$ ,  $p < 0.001$ ) were significantly correlated, further confirming that these two substances are major drivers in PHE rhizoremediation.

#### Reconstruction of PHE metabolic pathways and the relationships between their related genes and degradation efficiency

Based on GhostKOALA annotation and the AromaDeg database, PHE degradation pathways including phthalate/protocatechuate and naphthalene/salicylate were mapped (Fig. 6). Overall, although both the phthalate/

protocatechuate and salicylate pathways existed in all  $^{13}\text{C}$ -DNA metagenomes of the unplanted and planted treatments, they had different gene contents. The contents of all identified genes were significantly higher in the  $^{13}\text{C}$ -DNA metagenomes of planted rhizospheres, 6.93–8.33-fold higher than those of the unplanted microcosms (Fig. S12). Among the plant rhizospheres, RG exhibited the greatest increase in PHE degradation-related gene content ( $p < 0.05$ ), followed by TF and SG, consistent with the trend of PHE degradation. These results suggest the different rhizoremediation mechanisms across treatments. All 18 identified PHE degradation-related genes had higher contents in the  $^{13}\text{C}$ -DNA metagenomes of the RG rhizosphere; 11 of 18 genes (e.g. genes encoding PAH dioxygenase, salicylate hydroxylase, phthalate dioxygenase and

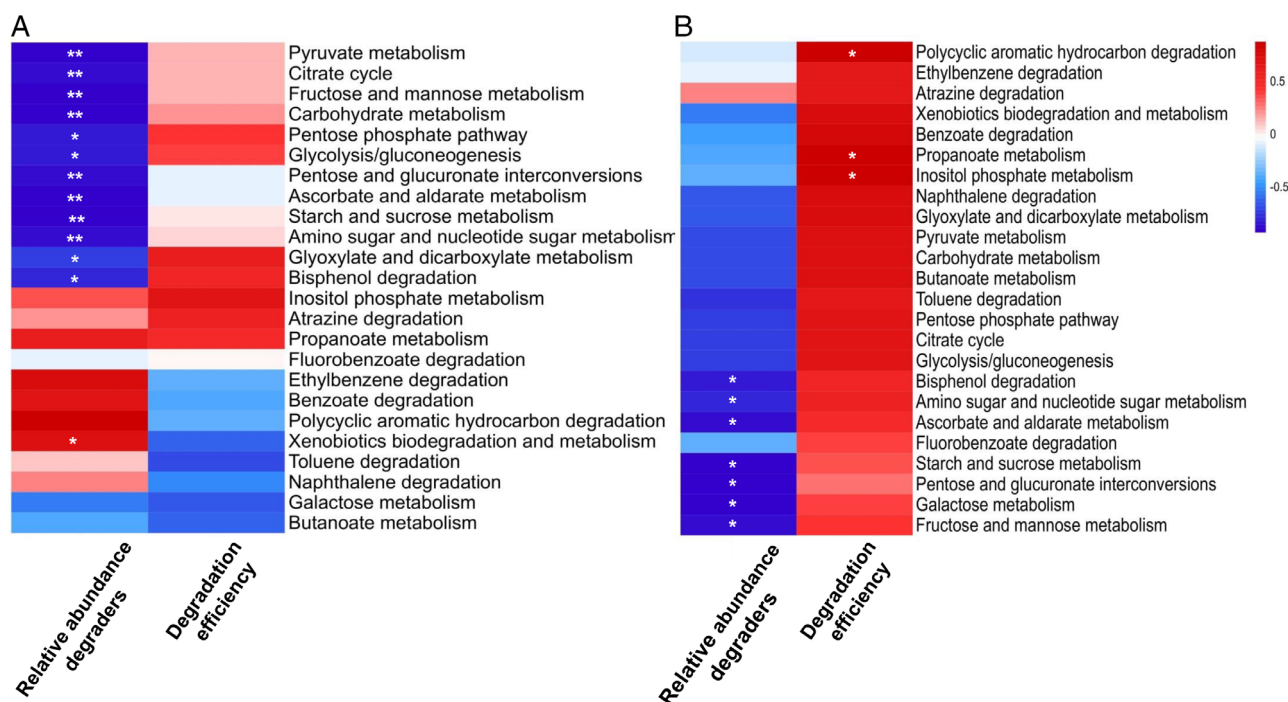


**Fig. 5.** Pearson correlations between the abundance (A) and number (B) of gene sequences affiliated to two functional categories (carbohydrates and xenobiotics biodegradation/metabolism) and the active phenanthrene degraders or degradation efficiencies. Colours indicate Pearson correlation coefficients, increasing from blue (low) to red (high). Values are means of three independent replicates. Single asterisk and double asterisk indicate significant correlations at the 0.05 and 0.01 levels respectively. [Color figure can be viewed at [wileyonlinelibrary.com](http://wileyonlinelibrary.com)]

protocatechuate dioxygenase) increased in all rhizosphere treatments (Fig. 6).

To more fully understand the differences in PHE degradation mechanisms across rhizospheres, we analysed the correlations between PHE degradation related genes and PHE degradation efficiency. As shown in Table S5, significant positive correlations were observed between PHE degradation efficiency and the total contents of genes involved in the PHE metabolic pathways ( $r = 0.974$ ,  $p < 0.05$ ), as well as PAH dioxygenase gene content ( $r = 0.951$ ,  $p < 0.05$ ). However, no significant correlations were observed between PHE degradation efficiency and the contents of other genes identified in the PHE metabolic pathways.

#### Co-occurrence ecological network

We performed additional analyses regarding the interactions between active PHE degraders and the other main OTUs across treatments after the 12-day incubation. As shown in Figs S13 and S14, an extremely complex connection within microbial communities was observed during the PHE biodegradation process in each treatment. Ecological networks in AD, RG, TF and SG microcosms consisted of 872 (51 nodes), 2800 (89 nodes), 2239 (83 nodes) and 1564 (71 nodes) pairs of significant correlations (false discovery rate-corrected  $p \leq 0.01$ )

respectively. MENA showed higher average degrees (avgK) in RG (62.9), TF (53.9) and SG (44.1) treatments than in AD microcosms (34.2), indicating that all planted treatments produced an obvious increase in the co-occurrence of soil microorganisms. In addition to the number of edges of all OTUs and avgK, the links between active PHE degraders and other core OTUs in the different microcosms were compared. In the planted soils, active PHE degraders showed markedly more links with the other main OTUs (780, 643 and 379 edges in the RG, TF and SG treatments respectively) than those in the unplanted controls (148 edges), consistent with the increasing PHE degradation efficiency.

To explore possible connections between ecological network complexity and PHE degradation performance in rhizospheres, we analysed the Pearson correlation coefficient between soil 16S rRNA gene, the active PHE degraders, PHE degradation-related genes and PHE degradation efficiency on avgK. As shown in Fig. S14d, the ecological network complexity was significantly correlated with the edges of all OTUs (Pearson correlation = 0.995,  $p < 0.01$ ), the active PHE degraders (Pearson correlation = 0.992,  $p < 0.01$ ), PHE degradation efficiency (Pearson correlation = 0.981,  $p < 0.05$ ) and the contents of PHE degradation related genes (Pearson correlation = 0.973,  $p < 0.05$ ). Additionally, the ecological network had strong correlations with the

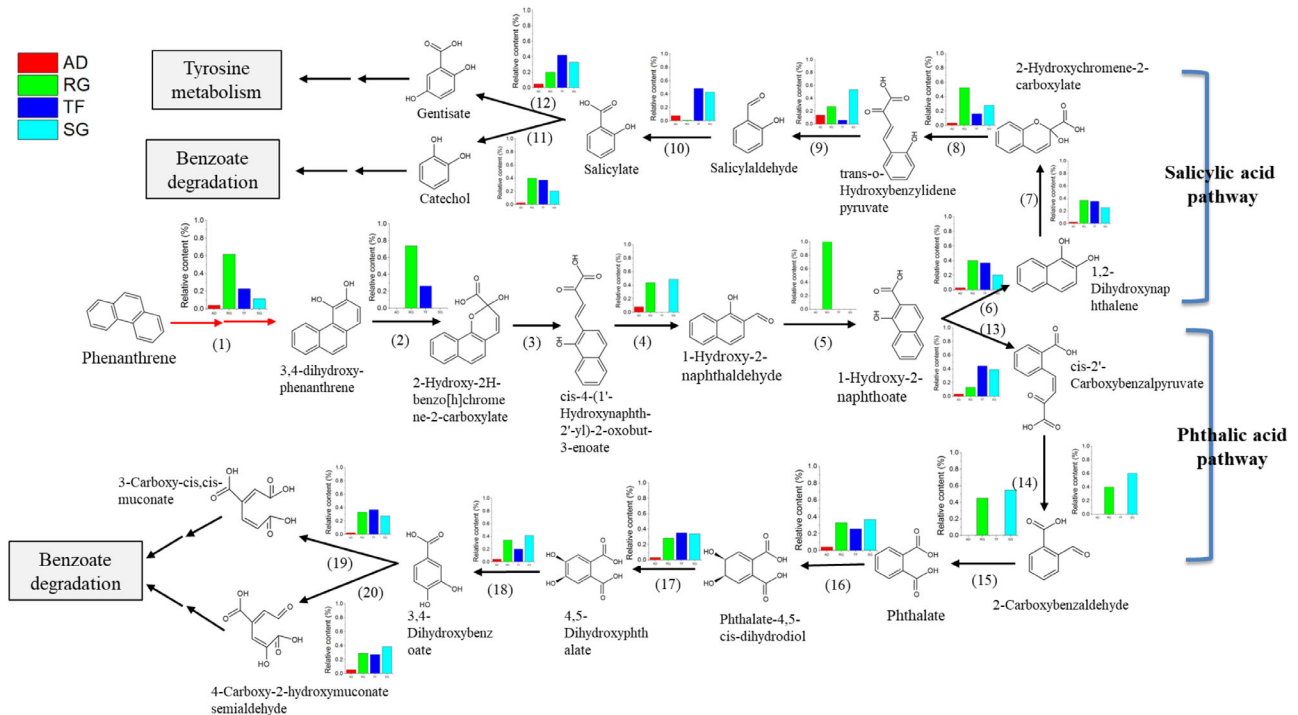


**Fig. 6.** Phenanthrene metabolic pathways in the unplanted and planted treatments. Red and black arrows represent the functional genes identified in the  $^{13}\text{C}$ -labelled metagenomes of different treatments using AromaDeg and GhostKOALA respectively. The histogram stands for the relative contents of genes encoding PHE metabolic enzymes in different treatments. The numbers stand for different enzymes as following: (1) PAH dioxygenase, (2) extradiol dioxygenase, (3) epimerase, (4) hydratase-aldolase, (5) aldehyde dehydrogenase, (6) salicylate hydroxylase, (7) 1,2-dihydroxynaphthalene dioxygenase, (8) 2-hydroxychromene-2-carboxylate isomerase, (9) trans-o-hydroxybenzylidene pyruvate hydratase-aldolase, (10) salicylaldehyde dehydrogenase, (11) salicylate hydroxylase (12) salicylate 5-hydroxylase, (13) 1-hydroxy-2-naphthoate dioxygenase (14) 4-(2-carboxyphenyl)-2-oxobut-3-enoate aldolase, (15) 2-formylbenzoate dehydrogenase, (16) phthalate 4,5-dioxygenase, (17) phthalate 4,5-cis-dihydrodiol dehydrogenase, (18) 4,5-dihydroxyphthalate decarboxylase, (19) protocatechuate 3,4-dioxygenase and (20) protocatechuate 4,5-dioxygenase. [Color figure can be viewed at [wileyonlinelibrary.com](http://wileyonlinelibrary.com)]

metabolisms of Pr (Pearson correlation = 0.93) and IP (Pearson correlation = 0.92), which were similar to the correlations with active degraders (Pearson correlation = 0.94).

#### Verification of Pr and IP to enhance PAH rhizoremediation

Similar to the results described in the section entitled 'Biodegradation of PHE', PHE degradation efficiencies in the planted soils were better than those in the unplanted treatments (Fig. S15). On day 6, supplements of Pr and IP did not show obvious enhancing effects on PHE degradation comparing to the microcosms without these two substrates. No significant differences ( $p > 0.05$ ) were observed among VRG, VRG\_Pr, VRG\_IP and VRG\_Pr\_IP treatments in terms of PHE degradation efficiency. However, after a 12-day incubation (Fig. S15), Pr or/and IP exhibited a significant decline of PHE concentration in the unplanted soils ( $p < 0.05$ ), comparing to VAD and VAD\_Pr\_IP treatments, which had the best performance, indicating that these two substances could promote PHE degradation in contaminated soils.

Approximately 39.7%, 34.8%, 36.6% and 32.9% of PHE remained in VAD, VAD\_Pr, VAD\_IP and VAD\_Pr\_IP microcosms after the 12-day incubation. In planted soils, the addition of these two substances also exhibited patterns similar to findings in the unplanted treatments. The residual PHE was significantly lower in VRG\_Pr (28.1%) and VRG\_Pr\_IP (26.2%) microcosms than in the VRG (31.0%) treatment ( $p < 0.05$ ). Accordingly, treatments supplemented with both Pr and IP exhibited the highest PHE degradation efficiency regardless the planation, followed by the microcosms with Pr or IP alone. This result further illustrated the critical roles of these two substances in accelerating PHE degradation.

#### Discussion

PAH degradation can be accelerated with the aid of rhizospheres in contaminated soils (Cheema *et al.*, 2010; Bandowe *et al.*, 2019). Here, soils planted with TF, RG or SG significantly increased the PHE removal efficiency, consistent with the findings of previous studies (Chen *et al.*, 2003; Cheema *et al.*, 2010). However, different plant rhizospheres exhibit distinct degradation

performances (Cheema *et al.*, 2010). Generally, higher PHE dissipation was found in treatments planted with RG compared to TF (Cheema *et al.*, 2010) or SG (Chen *et al.*, 2003). The improvement in PHE biodegradation was attributed to the rhizosphere effects of grasses (Li *et al.*, 2019b), because the plant rhizosphere could improve soil physiochemical properties and provide additional nutrients for the rhizospheric bacterial community during PAH degradation processes (Haichar *et al.*, 2008). Therefore, PAH rhizoremediation was accelerated by the populations and activities of soil microbes (Li *et al.*, 2019b). To explore the PAH rhizoremediation mechanisms, previous studies have typically focused on correlations of PAH degradation with the whole rhizosphere bacterial communities (Chen *et al.*, 2003; Shahsavari *et al.*, 2015; Li *et al.*, 2019b). However, few studies have linked active PAH-degrading microorganisms to rhizoremediation performance (Thomas *et al.*, 2019; Li *et al.*, 2019b). Here, SIP-metagenomics was first applied to assess and compare the influences of different prairie grasses on the diversity, composition and catabolic pathways of active PHE degraders in PAH-contaminated soils, and investigate the factors that drive the active PHE degraders. The results provide insights into the mechanisms of *in situ* rhizoremediation of PAH-contaminated soils and explain the mechanisms causing the difference across plant cultivars.

The abundance and diversity of active degraders are considered the dominant factors driving pollutant degradation (Li *et al.*, 2019b). The composition and abundance of active PHE degraders were altered as rhizosphere enriched and encouraged some indigenous PAH degraders (Li *et al.*, 2019b). Here, active PHE degraders in the planted and unplanted treatments were successfully identified by SIP. Among them, active degraders assigned to the classes *Alphaproteobacteria* and *Betaproteobacteria* were shared by all the planted and unplanted treatments (Fig. 3). *Erythrobacteraceae* (Yuan, 2015), *Erythrobacter* (Yuan, 2015), *Novosphingobium* (Fida *et al.*, 2017), *Sphingomonas* (Gong *et al.*, 2018), *Achromobacter* and *Burkholderia* (Revathy *et al.*, 2015; Izmalkova *et al.*, 2018) were able to degrade PHE and other PAHs; but PAHs biodegradation by *Pelagibius*, *Methylibium* and *Desulfuromonas* strains has not been previously reported. Thus their roles in PAH biodegradation remain unclear. This study provides the first evidence that *Pelagibius*, *Diaphorobacter* and *Methylibium* contribute to *in situ* PAH degradation. Additionally, many bacterial classes responsible for *in situ* PAH bioremediation have been found in  $\leq 3$  treatments, indicating that their roles in PHE degradation are altered by the rhizosphere. In these classes, *Marinobacter* (Wang *et al.*, 2017), *Alcanivorax* (Tiwari *et al.*, 2016), *Pseudomonas* (Sun *et al.*, 2019), *Stenotrophomonas* (Tiwari *et al.*,

2016) and *Mycobacterium* (Guo *et al.*, 2010) are known to degrade PHE and contain genes encoding the initial dioxygenases required for *in situ* PAH degradation. However, other degraders like *Tumebacillus*, *Citrobacter*, *Prostheco bacter* and *Thermomicrobia* were not previously reported to degrade PAHs; thus their roles in PAH metabolism are unclear. To our knowledge, this work is the first to reveal their PHE degradation capability, expanding the knowledge concerning functions of these bacterial taxa.

To better understand how the rhizosphere drives active PHE degraders in accelerating PHE rhizoremediation, it is necessary to profile and explore PHE-degradation related genes in various metabolic pathways (Thomas *et al.*, 2019). SIP-metagenomics are often used to compare microbiotas to assess the significant differences in the compositions of taxonomies, genes or functions (Chen and Murrell, 2010; Kraiselburd *et al.*, 2019; Thomas *et al.*, 2019), which help in reconstructing the PAH metabolic pathways in non-rhizospheric and rhizospheric soils. A previous study showed that the RG rhizosphere alone could shift the contribution of the active degraders to different degradation pathways of phthalate/protocatechuate and salicylate (Thomas *et al.*, 2019), similar to our results regarding  $^{13}\text{C}$ -DNA metagenomes in the RG rhizosphere. However, it remains unclear how the rhizospheres of other plants affect PHE degradation pathways. Here we successfully established the PHE degradation pathways of different rhizospheric soils. Although the key pathways involved in PHE degradation including phthalate/protocatechuate and salicylate pathways were all detected in non-rhizospheric and rhizospheric soils, the abundances and contents of genes responsible for these pathways varied. This result explained the distinct rhizoremediation mechanisms of different plants, which was also demonstrated by the positive correlations of PHE degradation efficiency with genes involved in the PHE metabolic pathways. Importantly, with the exception of the PAH dioxygenase gene, the contents of other genes involved in PHE metabolic pathways showed no significant correlations with PHE degradation efficiency, inferring the possible changes in metabolic pathways and metabolites between different rhizospheres.

In addition to the metabolic pathways of target pollutants, metagenomics can assess differences in other substance metabolisms (e.g. carbohydrates) and analyse their relationships with target pollutants (Zhang *et al.*, 2019; Li *et al.*, 2020b). Indeed, carbohydrate metabolisms are often associated with PAH degradation (Bourceret *et al.*, 2015; Thomas *et al.*, 2019). However, only one study has examined the role of carbohydrate metabolism in PHE degradation efficiency, compared between RG rhizosphere and non-rhizosphere soils (Thomas *et al.*, 2019); the findings indicated that carbohydrate catabolic genes were more

abundant in planted soils, where they possibly reduced the abundances of genes associated with PAH metabolism, then inhibited PAH degradation performance (Thomas *et al.*, 2019). Here, we found that carbohydrate metabolism could promote the growth of the active PHE degraders, as well as their PHE degradation efficiencies. More importantly, this is presumably the first report to identify Pr and IP as the dominant factors that drive active PHE degraders in rhizospheres. Although some carbohydrates such as inositol galactoside (Li *et al.*, 2021), sucrose (Li *et al.*, 2021), citric acid (Liao *et al.*, 2006) and fructose (Usyskin-Tonne *et al.*, 2020) were largely accumulated in plant rhizospheres and significantly changed the microbial community structure (Usyskin-Tonne *et al.*, 2020), the relationship between PAH degradation and carbohydrate metabolism (e.g. Pr and IP) has not been studied in rhizospheres. Thus, the mechanisms of PAH rhizoremediation driven by carbohydrates remain unclear. Pr is a low-molecular-weight organic acid that can be utilized by rhizospheric microbes (Koo *et al.*, 2005). It can accelerate the mineralisation of organic pollutants, such as tetrachloroethene and benzo(a)pyrene (Fennell *et al.*, 1997; N'Guessan *et al.*, 2004). However, no literature thus far has focused on the relationship between Pr and PAH degradation in rhizosphere. Additionally, organic phosphate in rhizosphere usually has connections with organic acids (Almeida *et al.*, 2018), which are exuded from plant roots and mobilize organic phosphate (e.g. IPs) as the dominant forms of organic phosphate in many soils (Turner *et al.*, 2002; Almeida *et al.*, 2018). The rhizosphere environment is reported to increase the biodegradation of IP (Almeida *et al.*, 2018), but no study has addressed IP metabolism during the rhizoremediation of organic pollutants. Here, we found that propionic acid and IPs metabolism processes have important roles in PHE rhizoremediation; they may be the main factors driving the active PHE degraders to remove PHE from contaminated soils. This was proven by the correlations of PHE degrader populations with Pr/IP metabolisms (Figs 5 & S11), implying their key roles in selecting and encouraging the rhizosphere PHE degraders. This conclusion was further confirmed by enhanced PAH rhizoremediation after Pr and IP supplementation (Fig. S15). Our findings expand the understanding regarding the mechanisms of PHE rhizoremediation driven by carbohydrates in contaminated soils.

Increasing reports of microbial interactions have led to a greater focus on the interrelationships between active degraders and other members within the community during the pollutant degradation processes, which is crucial to unravelling the mechanisms of *in situ* biodegradation and improving the degradation performance (Song *et al.*, 2019; Li *et al.*, 2020a). However, no study has explored such complex relationships in the plant

rhizosphere. The present study explored the link between the ecological network and PAH rhizoremediation; it showed that the complexity of links between active PHE degraders and other microbes was significantly correlated with PAH degradation and PHE degradation-related genes. This result hinted the contribution of rhizospheres to the enhanced connections between active PHE degraders and other microbes (Fig. S14d), consistent with previously reported associations of organic pollutant degradation with microbial interactions in non-rhizospheric environments (Song *et al.*, 2019; Li *et al.*, 2020a). In addition to their roles in promoting the populations of active PHE degraders, we found that the metabolism of some carbohydrates (e.g. Pr and IP) might simultaneously strengthen microbial connections within rhizospheres and conductively accelerate the rhizoremediation of organic pollutants. Our research is the first to elucidate associations among PHE degradation efficiency, active PHE degraders and bacterial interactions, offering a new perspective for the rhizoremediation mechanisms of environmental pollutants.

## Materials and methods

### Soil preparation and plant establishment

Soil was collected from Shengli Oil Field, China (37°68'N, 118°48'E), dried at room temperature, and sieved using a 2-mm sieve, as described in our previous study (Li *et al.*, 2019b). Then portions of soil samples for initial DNA extraction and chemical analyses were stored at -20°C. The remaining samples were placed at 4°C for SIP. The soil characteristics and PAH contents are listed in Table S1.

Three prairie grasses, RG (*Lolium perenne*), TF (*Festuca arundinacea*) and SG (*Panicum virgatum* L.), were selected because of their prior performance in the enhancement of PAH degradation in some field studies (Chen *et al.*, 2003; Li *et al.*, 2019b). Plant seeds were sterilized using 30% (vol./vol.) H<sub>2</sub>O<sub>2</sub> for 30 min and germinated in perlite at room temperature before transferring to Hoagland nutrient solution for further growth until the mature period according to our previous study (Li *et al.*, 2019b). The mature plants were prepared for the PHE biodegradation and SIP experiments.

### SIP incubation

SIP microcosms were performed in miniature planting pots as described by Li *et al.* (2019b). Briefly, unlabelled or <sup>13</sup>C-labelled PHE (<sup>13</sup>C<sub>14</sub>-PHE, 99%; Cambridge Isotope Laboratories, Tewksbury, MA, USA) was added to the soil samples at an initial concentration of 5 mg kg<sup>-1</sup>. After adjustment of the soil moisture content (60%, vol./

wt.) of the water-holding capacity, soil (5 g) was added to each spot and watered throughout the whole experiment to maintain consistent water content. For the planted microcosms, two uniform mature grasses were carefully transplanted from the nutrient solution to experimental pots and grown for 12 days.

In total, eight biotic treatments listed in Table S2 are designated as  $^{12}\text{C\_AD}$  ( $^{12}\text{C-PHE}$  alone),  $^{12}\text{C\_RG}$  ( $^{12}\text{C-PHE}$  with RG),  $^{12}\text{C\_TF}$  ( $^{12}\text{C-PHE}$  with TF),  $^{12}\text{C\_SG}$  ( $^{12}\text{C-PHE}$  with SG),  $^{13}\text{C\_AD}$  ( $^{13}\text{C-PHE}$  only),  $^{13}\text{C\_RG}$  ( $^{13}\text{C-PHE}$  with RG),  $^{13}\text{C\_TF}$  ( $^{13}\text{C-PHE}$  with TF) and  $^{13}\text{C\_SG}$  ( $^{13}\text{C-PHE}$  with SG). Non-bioactive treatment (CK) as a sterile control (SC) was also established using soils sterilized by gamma ray. Each treatment was tested with six replicates. For treatments with plants, individual plants were carefully dug out and the rhizosphere soils were collected by brushing the plant roots based on the method previously described (Deng *et al.*, 2018). All the treatments were cultured in a growth chamber at 28/22°C (day/night) with a 16 h/8 h photoperiod and relative humidity of 60% based on the methods described previously (Li *et al.*, 2019b). After 6 and 12 days of incubation, soil samples from each microcosm were collected for chemical analyses and DNA extraction.

#### DNA extraction, ultracentrifugation, 16S rRNA gene amplicon sequencing and analyses

Extended details for this section are provided in the Supporting Information. Briefly, DNA taken on days 6 and 12 from each treatment was selected for ultracentrifugation. After quantification with an ultraviolet–visible spectrophotometer (ND-2000), the extracted DNA (approximately 5 µg) mixed with a CsCl solution prepared in Tris-EDTA (pH 8.0), with a final BD of  $\sim 1.77 \text{ g ml}^{-1}$  was ultracentrifuged at 45 000 rpm for 48 h at 20°C as previously described (Li *et al.*, 2020a). After ultracentrifugation, the products were fractionated and purified (Li *et al.*, 2019b). For amplicon sequencing, the hypervariable V4 region was amplified for the DNA fractions derived from all treatments using the primer set 515f/806r (BGI, Beijing, China) (Li *et al.*, 2018b). PCR was performed in accordance with our published method (Li *et al.*, 2019a). After purification and quantification, PCR products were sequenced on the Illumina MiSeq PE250, and sequences were subsequently analysed in QIIME and assigned to OTUs at a cut-off value of 97% to generate microbiome profiles (Edgar, 2010; Werner *et al.*, 2012).

To detect the active PHE degraders, the relative abundance of each OTU in all samples amended with  $^{12}\text{C-PHE}$  or  $^{13}\text{C-PHE}$  was calculated; the top 100 OTUs were selected for further analyses (Li *et al.*, 2017). Active degraders involved in *in situ* PHE metabolism were

characterized by assessing the relative abundances of specific OTUs in the  $^{13}\text{C-PHE}$  microcosms compared with those specific OTUs in the  $^{12}\text{C-PHE}$  microcosms from each fraction. Phylogenetic information of the identified PHE degraders was performed as previously described (Li *et al.*, 2014).

#### Real-time quantitative PCR

The bacterial 16S rRNA genes in each fraction from  $^{13}\text{C-PHE}$  and  $^{12}\text{C-PHE}$  amended microcosms were amplified using the specific primer set Bac519F/Bac907R, as in our previous work (Li *et al.*, 2018a). The qPCR reactions and conditions were implemented using the previously described process (Li *et al.*, 2019b). After gel purification, the PCR products were cloned into the pGEM-T plasmid vector and sequenced. Fractions identified as the ‘heavy’ DNA ( $^{13}\text{C-DNA}$ ) had a BD of  $1.755\text{--}1.756 \text{ g m}^{-1}$  and were determined jointly by both 16S rRNA high-throughput sequencing and qPCR analyses.

#### Metagenomic sequencing and analyses

The  $^{13}\text{C-DNA}$  recovered from  $^{13}\text{C\_AD}$ ,  $^{13}\text{C\_RG}$ ,  $^{13}\text{C\_TF}$  and  $^{13}\text{C\_SG}$  microcosms on day 12 were sequenced by the Illumina HiSeq X-ten platform (Illumina, USA) with PE150 strategy at Personal Biotechnology (Shanghai, China). On average, 10 Gb data were generated for each sample (120 Gb in total). The sequencing adapters were removed, and the reads were trimmed using the sliding window scanning method with default settings in Trimmomatic (version 0.33) (Bolger *et al.*, 2014). Sequences were then filtered to remove too short reads (<80 nucleotides) and the reads with a mean quality score <25. Human contamination was further removed (Blastn *E*-value threshold  $\leq 10^{-5}$ , bitscore  $\geq 50$ , percentage identity  $\geq 75\%$ ) by mapping the reads against the human reference genome (build 37) using bowtie2 (version 2.1.0) (Langmead *et al.*, 2009). Subsequently, the short sequence data were assembled into high-quality contigs by the MEGAHIT assembler (Li *et al.*, 2015). Totally, 86 509–144 401 assembled contigs longer than 1000 bp were used for open reading frame prediction with software Prodigal. Then protein sequence was annotated for each sample using eggNOG-mapper (Huerta-Cepas *et al.*, 2019). Clean short sequences were also aligned to the UniRef90 database and the KEGG metabolic pathway abundances in planted and unplanted treatments were inferred using the software HUMAnN2 (Abubucker *et al.*, 2012). Functional genes potentially involved in the aerobic degradation of aromatic compounds were screened using the AromaDeg database with the following alignment parameters: *E*-value >0.00001, identity >50%, query coverage >50%, subject

coverage >30% (Thomas *et al.*, 2019). The resulting sequences associated with AromaDeg enzyme families were subsequently aligned using MAFFT with an L-INS-i strategy (Katoh *et al.*, 2005) and edited using JalView 2 (Waterhouse *et al.*, 2009). Phylogenetic analyses of these alignments were conducted as previously described (Li *et al.*, 2014). Genes involved in the carbohydrate metabolism were annotated using carbohydrate-active enzymes database (Lombard *et al.*, 2013). Note that because the KEGG database only contains *nahAc* and *nidA* genes from microbes such as *Pseudomonas* and *Mycobacterium*, GhostKOALA could not recognize the genes involved in the first steps of PHE degradation from the identified PHE degraders. Thus, both KEGG and AromaDeg databases were used to reconstruct the metabolic pathways of PAH degraders in the <sup>13</sup>C-DNA metagenomes of unplanted and planted treatments as described by Thomas *et al.* (2019). All sequencing data were submitted to NCBI (PRJNA721029).

#### Chemical analyses

PHE in soils and plant tissues was extracted from each treatment containing unlabelled PHE (days 6 and 12 after incubation) and analysed by GC-MS (Agilent 7890) as previously described (Li *et al.*, 2019a; Li *et al.*, 2019b). Briefly, the samples were spiked with recovery standards and extracted using dichloromethane. After purification by a silica-gel/alumina column, the organic extract was concentrated to ~0.5 ml. Before instrumental analyses, 1000 ng hexamethylbenzene was added to the organic solvents as an internal standard.

#### Ecological network

Ecological network was performed using MENA pipeline to explore interspecies interactions among different microbial lineages, particularly concerning active PHE degraders and other members within the community in the rhizosphere and non-rhizosphere soils, as previously described (Deng *et al.*, 2012). OTUs appearing in all treatments, which exhibited the relative abundance greater than 0.1% or were identified by SIP as active PHE degraders, were used to construct the ecological network. Pearson correlation analysis was applied to detect associations between each OTU and the threshold was determined via a random matrix theory-based method.

#### Verification of Pr and IP in enhancing PAH rhizoremediation

Considering that RG exhibited the highest PHE degradation efficiency, we selected RG as the representative

plant to verify the enhancing effects of Pr and IP on PAH degradation in the rhizospheres. Microcosms were established in the pots by means of the same protocol used in the SIP incubations. To prepare the inoculum, propanoate (Pr) or inositol 1-phosphate (IP) was added into the bottles at a final concentration of 30 mg kg<sup>-1</sup>. Nine treatments including a SC established using soils sterilized by gamma ray, VAD (<sup>12</sup>C-PHE-supplemented soil alone), VAD\_Pr (<sup>12</sup>C-PHE-supplemented soil with Pr), VAD\_IP (<sup>12</sup>C-PHE-supplemented soil with IP), VAD\_Pr\_IP (<sup>12</sup>C-PHE-supplemented soil with both Pr and IP), VRG (<sup>12</sup>C-PHE-supplemented soil with RG), VRG\_Pr (<sup>12</sup>C-PHE-supplemented soil with RG and Pr), VRG\_IP (<sup>12</sup>C-PHE-supplemented soil with RG and IP), VRG\_Pr\_IP (<sup>12</sup>C-PHE-supplemented soil with RG, Pr and IP), were tested. Each treatment was performed in six replicates, and chemical analyses were performed as described in the 'Chemical analyses' section.

#### Statistical analyses

Data were calculated using Microsoft Excel 2013 and expressed as the mean ± standard deviation. Statistical analyses were performed using Origin 8.0 (OriginLab Corporation, Northampton, MA, USA), SPSS 17.0 (SPSS, Chicago, IL, USA) and R (version 4.0.0; R Foundation for Statistical Computing, Vienna, Austria) with a significance of  $p = 0.05$ . Phylogenetic information regarding the gene sequences of active degraders was analysed using the basic local alignment search tool algorithm (National Center for Biotechnology Information, Bethesda, MD, USA) and MEGA version 4.0. Pearson correlation analysis between the abundance of pathways and other measurements (active PHE degrader abundance and degradation efficiency) was performed using the *trans\_env* class of the R *microeco* package (Liu *et al.*, 2021).

#### Acknowledgements

Financial support was provided by the National Natural Science Foundation of China (No. 32061133003 & 41907298), the Key-Area Research and Development Program of Guangdong Province (2020B1111530003) and the Natural Science Foundation of Guangdong Province, China (2021A1515011561 & 2019A1515011862). This article was also granted by the Tuguangchi Award for Excellent Young Scholar GIGCAS and the State Key Laboratory of Organic Geochemistry, GIGCAS (Grant No. SKLOG2020-8).

#### References

Abubucker, S., Segata, N., Goll, J., Schubert, A.M., Izard, J., Cantarel, B.L., *et al.* (2012) Metabolic reconstruction for

- metagenomic data and its application to the human microbiome. *PLoS Comp Biol* **8**: e1002358.
- Almeida, D.S., Menezes-Blackburn, D., Turner, B.L., Wearing, C., Haygarth, P.M., and Rosolem, C.A. (2018) *Urochloa ruziziensis* cover crop increases the cycling of soil inositol phosphates. *Biol Fertil Soils* **54**: 935–947.
- Amann, R.I., Ludwig, W., and Schleifer, K.H. (1995) Phylogenetic identification and in situ detection of individual microbial cells without cultivation. *Microbiol Rev* **59**: 143–169.
- Bandowe, B.A.M., Leimer, S., Meusel, H., Velescu, A., Dassen, S., Eisenhauer, N., et al. (2019) Plant diversity enhances the natural attenuation of polycyclic aromatic compounds (PAHs and oxygenated PAHs) in grassland soils. *Soil Biol Biochem* **129**: 60–70.
- Bolger, A.M., Lohse, M., and Usadel, B. (2014) Trimmomatic: a flexible trimmer for Illumina sequence data. *Bioinformatics* **30**: 2114–2120.
- Bourceret, A., Leyval, C., de Fouquet, C., and Cebon, A. (2015) Mapping the centimeter-scale spatial variability of PAHs and microbial populations in the rhizosphere of two plants. *PLoS One* **10**: e0142851.
- Cheema, S.A., Imran Khan, M., Shen, C., Tang, X., Farooq, M., Chen, L., et al. (2010) Degradation of phenanthrene and pyrene in spiked soils by single and combined plants cultivation. *J Hazard Mater* **177**: 384–389.
- Chen, Y., and Murrell, J.C. (2010) When metagenomics meets stable-isotope probing: progress and perspectives. *Trends Microbiol* **18**: 157–163.
- Chen, Y.C., Banks, M.K., and Schwab, A.P. (2003) Pyrene degradation in the rhizosphere of tall fescue (*Festuca arundinacea*) and switchgrass (*Panicum virgatum* L.). **37**: 5778–5782.
- Deng, S., Ke, T., Li, L., Cai, S., Zhou, Y., Liu, Y., et al. (2018) Impacts of environmental factors on the whole microbial communities in the rhizosphere of a metal-tolerant plant: *Elsholtzia haichowensis* Sun. *Environ Pollut* **237**: 1088–1097.
- Deng, Y., Jiang, Y.-H., Yang, Y., He, Z., Luo, F., and Zhou, J. (2012) Molecular ecological network analyses. *BMC Bioinformatics* **13**: 113.
- Edgar, R.C. (2010) Search and clustering orders of magnitude faster than BLAST. *Bioinformatics* **26**: 2460–2461.
- Fennell, D.E., Gossett, J.M., and Zinder, S.H. (1997) Comparison of butyric acid, ethanol, lactic acid, and propionic acid as hydrogen donors for the reductive dechlorination of tetrachloroethene. *Environ Sci Technol* **31**: 918–926.
- Fida, T.T., Moreno-Forero, S.K., Breugelmans, P., Heipieper, H.J., Roling, W.F.M., and Springael, D. (2017) Physiological and transcriptome response of the polycyclic aromatic hydrocarbon degrading *Novosphingobium* sp LH128 after inoculation in soil. *Environ Sci Technol* **51**: 1570–1579.
- Gong, B., Wu, P., Bo, R., Zhang, Y., and Dang, Z. (2018) Differential regulation of phenanthrene biodegradation process by kaolinite and quartz and the underlying mechanism. *J Hazard Mater* **349**: 51–59.
- Guo, C., Dang, Z., Wong, Y., and Tam, N.F. (2010) Biodegradation ability and dioxygenase genes of PAH-degrading *Sphingomonas* and *Mycobacterium* strains isolated from mangrove sediments. *Int Biodeterior Biodegrad* **64**: 419–426.
- Guo, M.X., Gong, Z.Q., Miao, R.H., Rookes, J., Cahill, D., and Zhuang, J. (2017) Microbial mechanisms controlling the rhizosphere effect of ryegrass on degradation of polycyclic aromatic hydrocarbons in an aged-contaminated agricultural soil. *Soil Biol Biochem* **113**: 130–142.
- Haichar, F.Z., Marol, C., Berge, O., Rangelcastro, J.I., Prosser, J.I., Balesdent, J., et al. (2008) Plant host habitat and root exudates shape soil bacterial community structure. *ISME J* **2**: 1221–1230.
- Huerta-Cepas, J., Szklarczyk, D., Heller, D., Hernandez-Plaza, A., Forslund, S.K., Cook, H., et al. (2019) eggNOG 5.0: a hierarchical, functionally and phylogenetically annotated orthology resource based on 5090 organisms and 2502 viruses. *Nucleic Acids Res* **47**: D309–D314.
- Izmalkova, T.Y., Gafarov, A.B., Sazonova, O.I., Sokolov, S. L., and Boronin, A.M. (2018) Diversity of oil-degrading microorganisms in the Gulf of Finland (Baltic Sea) in spring and in summer. *Microbiology* **87**: 261–271.
- Katoh, K., Kuma, K.-I., Toh, H., and Miyata, T. (2005) MAFFT version 5: improvement in accuracy of multiple sequence alignment. *Nucleic Acids Res* **33**: 511–518.
- Koo, B.J., Adriano, D.C., Bolan, N.S., and Barton, C.D. (2005) Root exudates and microorganisms. In *Encyclopedia of Soils in the Environment*, Hillel, D. (ed). Oxford: Elsevier, pp. 421–428.
- Kraiselburd, I., Bruels, T., Heilmann, G., Kaschani, F., Kaiser, M., and Meckenstock, R.U. (2019) Metabolic reconstruction of the genome of candidate *Desulfatiglans* TRIP\_1 and identification of key candidate enzymes for anaerobic phenanthrene degradation. *Environ Microbiol* **21**: 1267–1286.
- Kuppusamy, S., Thavamani, P., Singh, S., Naidu, R., and Megharaj, M. (2016) Polycyclic aromatic hydrocarbons (PAHs) degradation potential, surfactant production, metal resistance and enzymatic activity of two novel cellulose-degrading bacteria isolated from koala faeces. *Environ Earth Sci* **76**: 14.
- Langmead, B., Trapnell, C., Pop, M., and Salzberg, S.L. (2009) Ultrafast and memory-efficient alignment of short DNA sequences to the human genome. *Genome Biol* **10**: R25.
- Li, D.H., Liu, C.M., Luo, R.B., Sadakane, K., and Lam, T.W. (2015) MEGAHIT: an ultra-fast single-node solution for large and complex metagenomics assembly via succinct de Bruijn graph. *Bioinformatics* **31**: 1674–1676.
- Li, J., Lin, T., Lu, Q., Wang, J.J., Liao, C., Pan, Y., and Zhao, Y. (2014) Changes in physicochemical properties and bactericidal efficiency of acidic electrolyzed water ice and available chlorine decay kinetics during storage. *LWT-Food Sci Technol* **59**: 43–48.
- Li, J., Luo, C., Song, M., Dai, Q., Jiang, L., Zhang, D., and Zhang, G. (2017) Biodegradation of phenanthrene in polycyclic aromatic hydrocarbon-contaminated wastewater revealed by coupling cultivation-dependent and -independent approaches. *Environ Sci Technol* **51**: 3391–3401.
- Li, J., Luo, C., Zhang, D., Cai, X., Jiang, L., and Zhang, G. (2019a) Stable-isotope probing enabled cultivation of the indigenous strain *Ralstonia* sp. M1 capable of degrading phenanthrene and biphenyl in industrial wastewater. *Appl Environ Microbiol* **85**: e00511-19.

- Li, J., Luo, C., Zhang, D., Cai, X., Jiang, L., Zhao, X., and Zhang, G. (2019b) Diversity of the active phenanthrene degraders in PAH-polluted soil is shaped by ryegrass rhizosphere and root exudates. *Soil Biol Biochem* **128**: 100–110.
- Li, J., Luo, C., Zhang, D., Song, M., Cai, X., Jiang, L., and Zhang, G. (2018b) Autochthonous bioaugmentation modified bacterial diversity of phenanthrene degraders in PAH-contaminated wastewater as revealed by DNA-stable isotope probing. *Environ Sci Technol* **52**: 2934–2944.
- Li, J., Luo, C., Zhang, G., and Zhang, D. (2018a) Coupling magnetic-nanoparticle mediated isolation (MMI) and stable isotope probing (SIP) for identifying and isolating the active microbes involved in phenanthrene degradation in wastewater with higher resolution and accuracy. *Water Res* **144**: 226–234.
- Li, J., Peng, K., Zhang, D., Luo, C., Cai, X., Wang, Y., and Zhang, G. (2020a) Autochthonous bioaugmentation with non-direct degraders: a new strategy to enhance wastewater bioremediation performance. *Environ Int* **136**: 105473.
- Li, J.Y., Jin, X.Y., Zhang, X.C., Chen, L., Liu, J.L., Zhang, H. M., et al. (2020b) Comparative metagenomics of two distinct biological soil crusts in the Tengger Desert, China. *Soil Biol Biochem* **140**: 107637.
- Li, X., Ma, X., Cheng, Y., Liu, J., Zou, J., Zhai, F., et al. (2021) Transcriptomic and metabolomic insights into the adaptive response of *Salix viminalis* to phenanthrene. *Chemosphere* **262**: 27573–27573.
- Liao, Y.C., Chien, S.W.C., Wang, M.C., Shen, Y., Hung, P. L., and Das, B. (2006) Effect of transpiration on Pb uptake by lettuce and on water soluble low molecular weight organic acids in rhizosphere. *Chemosphere* **65**: 343–351.
- Liu, C., Cui, Y.M., Li, X.Z., and Yao, M.J. (2021) microeco: an R package for data mining in microbial community ecology. *FEMS Microbiol Ecol* **97**: fiae255.
- Lombard, V., Golaconda Ramulu, H., Drula, E., Coutinho, P. M., and Henrissat, B. (2013) The carbohydrate-active enzymes database (CAZy) in 2013. *Nucleic Acids Res* **42**: D490–D495.
- Luo, C., Zhao, X., Zhang, D., Dai, Y., Li, Q., Wang, S., et al. (2021) Toward a more comprehensive understanding of autochthonous bioaugmentation (ABA): cases of ABA for phenanthrene and biphenyl by *Ralstonia* sp. M1 in industrial wastewater. *ACS ES&T Water* **1**: 1390–1400.
- N'Guessan, A.L., Levitt, J.S., and Nyman, M.C. (2004) Remediation of benzo(a)pyrene in contaminated sediments using peroxy-acid. *Chemosphere* **55**: 1413–1420.
- Revathy, T., Jayasri, M.A., and Suthindhiran, K. (2015) Biodegradation of PAHs by *Burkholderia* sp. VITRSB1 isolated from marine sediments. *Scientifica* **2015**: 867586.
- Rochman, F.F., Sheremet, A., Tamas, I., Saidi-Mehrabad, A., Kim, J.-J., Dong, X., et al. (2017) Benzene and naphthalene degrading bacterial communities in an oil sands tailings pond. *Front Microbiol* **8**: 1845.
- Seo, J.S., Keum, Y.S., and Li, Q.X. (2009) Bacterial degradation of aromatic compounds. *Int J Environ Res Public Health* **6**: 278–309.
- Shahsavari, E., Adetutu, E.M., Taha, M., and Ball, A.S. (2015) Rhizoremediation of phenanthrene and pyrene contaminated soil using wheat. *J Environ Manage* **155**: 171–176.
- Song, M., Luo, C., Jiang, L., Peng, K., Zhang, D., Zhang, R., et al. (2019) The presence of in situ sulphamethoxazole degraders and their interactions with other microbes in activated sludge as revealed by DNA stable isotope probing and molecular ecological network analysis. *Environ Int* **124**: 121–129.
- Sun, S.L., Wang, Y.X., Zang, T.T., Wei, J.Y., Wu, H.Z., Wei, C.H., et al. (2019) A biosurfactant-producing *Pseudomonas aeruginosa* S5 isolated from coking wastewater and its application for bioremediation of polycyclic aromatic hydrocarbons. *Bioresour Technol* **281**: 421–428.
- Thomas, F., Corre, E., and Cebon, A. (2019) Stable isotope probing and metagenomics highlight the effect of plants on uncultured phenanthrene-degrading bacterial consortium in polluted soil. *ISME J* **13**: 1814–1830.
- Tiwari, B., Manickam, N., Kumari, S., and Tiwari, A. (2016) Biodegradation and dissolution of polyaromatic hydrocarbons by *Stenotrophomonas* sp. *Bioresour Technol* **216**: 1102–1105.
- Turner, B.L., Paphazy, M.J., Haygarth, P.M., and McKelvie, I. D. (2002) Inositol phosphates in the environment. *Philos Trans R Soc London Ser B Biol Sci* **357**: 449–469.
- Usyskin-Tonne, A., Hadar, Y., Yermiyahu, U., and Minz, D. (2020) Elevated CO<sub>2</sub> and nitrate levels increase wheat root-associated bacterial abundance and impact rhizosphere microbial community composition and function. *Isme J* **15**: 1073–1084.
- Wang, C.Y., Guo, G., Huang, Y., Hao, H., and Wang, H. (2017) Salt adaptation and evolutionary implication of a nah-related PAHs dioxygenase cloned from a halophilic phenanthrene degrading consortium. *Sci Rep* **7**: 12525.
- Waterhouse, A.M., Procter, J.B., Martin, D.M.A., et al. (2009) Jalview Version 2 – a multiple sequence alignment editor and analysis workbench. *Bioinformatics* **25**: 1189–1191.
- Werner, J.J., Koren, O., Hugenholtz, P., Desantis, T.Z., Walters, W.A., Caporaso, J.G., et al. (2012) Impact of training sets on classification of high-throughput bacterial 16s rRNA gene surveys. *ISME J* **6**: 94–103.
- Wu, Y., Ding, Q., Zhu, Q., Zeng, J., Ji, R., Dumont, M.G., and Lin, X. (2018) Contributions of ryegrass, lignin and rhamnolipid to polycyclic aromatic hydrocarbon dissipation in an arable soil. *Soil Biol Biochem* **118**: 27–34.
- Yu, X.Z., Wu, S.C., Wu, F.Y., and Wong, M.H. (2011) Enhanced dissipation of PAHs from soil using mycorrhizal ryegrass and PAH-degrading bacteria. *J Hazard Mater* **186**: 1206–1217.
- Yuan, J. (2015) The diversity of PAH-degrading bacteria in a deep-sea water column above the southwest Indian ridge. *Front Microbiol* **6**: 853.
- Zhang, Y., Ying, H.M., and Xu, Y.Z. (2019) Comparative genomics and metagenomics of the metallomes. *Metallomics* **11**: 1026–1043.

## Supporting Information

Additional Supporting Information may be found in the online version of this article at the publisher's web-site:

**Appendix S1:** Supporting information.